



## System Engineering Approaches for Enhancing the Structural Integrity and Operational Efficiency of CNC Machining Centers: A Numerical Simulation Study



Simone Pazzaglia<sup>1</sup>, Ana Pavlovic<sup>1</sup>, Dragan Marinkovic<sup>2</sup>, Cristiano Fragassa<sup>1\*</sup>

<sup>1</sup> Department of Industrial Engineering, University of Bologna, 40133 Bologna, Italy

<sup>2</sup> Institute of Mechanics, Technical University of Berlin, 10623 Berlin, Germany

\* Correspondence: Cristiano Fragassa (cristiano.fragassa@unibo.it)

Received: 02-01-2025

Revised: 02-25-2025

Accepted: 03-05-2025

**Citation:** S. Pazzaglia, A. Pavlovic, D. Marinkovic, and C. Fragassa, "System engineering approaches for enhancing the structural integrity and operational efficiency of CNC machining centers: A numerical simulation study," *J. Eng. Manag. Syst. Eng.*, vol. 4, no. 1, pp. 39–49, 2025. <https://doi.org/10.56578/jemse040103>.



© 2025 by the author(s). Licensee Acadlore Publishing Services Limited, Hong Kong. This article can be downloaded for free, and reused and quoted with a citation of the original published version, under the CC BY 4.0 license.

**Abstract:** This study investigates the application of numerical simulations to optimize the design and operational performance of CNC machining centers, with a focus on enhancing their structural integrity and durability. The primary objective is to identify design modifications that can mitigate the risks associated with mechanical impacts and extend the service life of the machines. Finite Element Method (FEM) simulations are conducted on actual CNC machines to examine their structural responses under a range of real-world impact scenarios. The simulations reveal critical stress concentrations and deformation patterns that occur in operational environments, providing valuable insights into the dynamic behavior of the machines. A system engineering approach is employed to simplify the analysis of the machine's response to these dynamic conditions, allowing for an efficient evaluation of potential design improvements. Linear static analyses, incorporating imposed deformation conditions, are used to gain a deeper understanding of the machine's structural weaknesses. Several model simplifications are introduced, including modifications to geometry, contact conditions, and material properties, ensuring that the quality and accuracy of the numerical models are maintained. The results highlight the potential for targeted design modifications to reduce the likelihood of mechanical failure and enhance operational efficiency. These findings suggest that the application of advanced computational mechanics can substantially improve machine performance, ultimately contributing to the longevity and reliability of CNC machining centers.

**Keywords:** Engineering simulations; Machine design optimization; Computational mechanics; CNC machining centers; Impact analysis; Structural simulations

### 1 Introduction

In the field of high-precision machining, the natural trend of progress is moving toward increasingly flexible, precise, efficient, safe and fast manufacturing systems [1–3]. This is achieved, among other factors, by designing lightweight yet rigid structures [4] that allow moving components, such as spindles, to operate at high speeds while being as efficient as possible [5]. A significant part of success is also ensured by the precision achieved through alignment and guiding systems. These highly refined kinematic systems, however, do not always respond well to unexpected events, such as an impact [6]. This type of issue has been analysed here in relation to a specific case.

To address impact-related issues, a finite element structural analysis (FEM) is proposed to study the machine, as in similar situations [7, 8]. This type of analysis enables the prediction of the structural behaviour during impacts, focusing on identifying the machine's most vulnerable components [9]. The intent is to establish a framework to explore these critical areas, assess the structural components that are weakest when impacted by the machine's operating head [10], and, finally, investigate the effect on the manufacturing process [11].

The simulation will allow for later refinement of intervention strategies, potentially including a structural redesign of critical elements or the introduction of yielding joints to mitigate impact effects [12].

The present study starts with defining plausible impact scenarios to ascertain critical geometries, which will represent the expected load conditions for further investigation. The initial phase includes an analysis of the entire

machine using CAD drawings, transitioning to simulation exercises. Static simulations, despite simplifying the dynamic nature of impacts, provide valuable insights into the structural response, highlighting areas of tension and deformation. This helps identify critical components for focused analysis and subsequent detailed study.

## 2 Materials and Methods

### 2.1 System

The system under investigation is a CNC machining center, designed and manufactured by SCM Group S.p.a., and known by the commercial name of ROUTECH Chronos [13]. It is a CNC machine tool designed for universal milling, capable of processing various lightweight, non-metallic materials to produce components used in nautical and aeronautical furnishings, caravans, molds, ladders, period furniture, and plastic products.

Featuring a rigid gantry-style framework with a mobile crossbeam, it ensures high precision and quality in machined parts while maintaining compact workspace requirements and maximizing accessibility (Figure 1). The center is equipped with a high-performance electro-spindle, accommodating intricate five-axis milling operations. Specifically, the X-axis and Y-axis correspond to the translational movements of the overhead carriage relative to the machine base, while the Z-axis controls the downward movement of the spindle along the vertical direction, allowing it to approach the work surface. Additionally, the two rotary axes include the A-axis, responsible for tilting movements around the X-axis, and the C-axis, enabling rotational motion around the Z-axis.

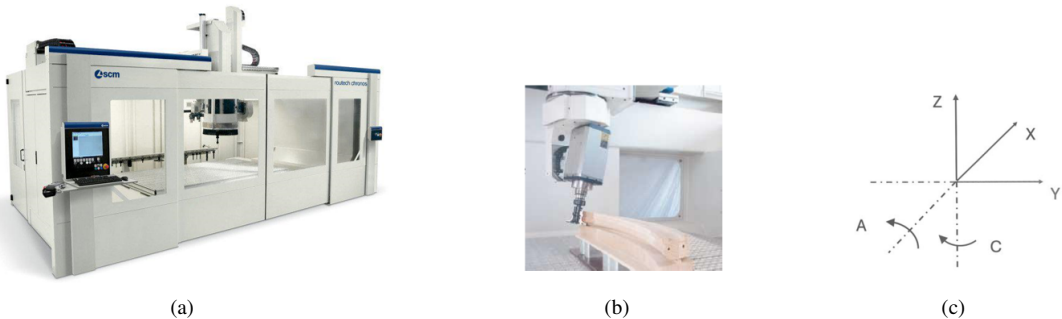


**Figure 1.** CNC machine tool under investigation: (a) Overview; (b) Working area; (c) Five-axis movements

This design approach enables the CNC machine to achieve rapid and precise machining across large work volumes, enhancing both productivity and safety with features such as polycarbonate doors and a fixed central bulkhead for secure pendulum machining. The technical specifications and main operational parameters are outlined in Table 1.

**Table 1.** Main technical characteristics of the CNC machine

Characteristics	Value
Axis travels (max)	5100 × 2200 × 1000 mm
Speed allowed X - Y	150 m/min(X/Y-axis) 75 m/min(Z-axis)
Working volume	4600 × 1700 × 900 mm
Rotation speed	1500 – 35000 rpm

The system is designed for diverse processing tasks due to its flexibility and the high degree of mobility provided by its 5 controlled axes. However, due to operator inexperience, the machine is often used as if it were a simpler 3-axis tool, leading to misuse and management challenges, particularly with complex movements.

Technical support reports indicate frequent instances where improper use results in the operating head suffering significant impacts. These incidents typically stem from incorrect programming of the tool path that fails to consider the dimensions of the electrospindle, with impacts occurring mainly during processing at low speeds, thus inducing minimal stress. Additionally, collisions often result from obstacles left on the tool path or from operator errors during setup. Such impacts generally lead to a loss of machine precision, prompting technicians to realign axes and inspect for possible structural damage that could affect functionality [14].

Moreover, support interventions usually occur early in the machine's operational phase when it is still new, with client companies expecting repair costs to be covered under warranty. This poses significant financial and reputational risks for the company, especially in an international market, complicating warranty claims when malfunctions are not clearly attributable to design flaws.

## 2.2 Modelling

The Pro-E CAD geometric modeler and Ansys Workbench [15] have been used as software tools through a workflow consisting of (a) geometry, (b) mesh, (c) materials, (d) contacts as follows.

### 2.2.1 Geometry

The CAD drawings have been analysed to identify functional groups and design complexity as follows:

- Base: load-bearing structure supporting the overhead carriage and all moving components.
- Overhead Carriage - enables movement along the X-axis and houses the tool magazine beneath it.
- Y-axis carriage system - allows motion along the Y-axis.
- Z-axis carriage system - facilitates vertical translation of the operating head.
- C-axis system - provides an angular excursion of  $640^\circ$  through a kinematic chain composed of a motor and a corresponding reducer, positioned at the base of the Z-carriage. Inside, it also contains the kinematic chain responsible for moving the second rotary axis.
- A-axis system - controls the rotation of the spindle, with an angular excursion capability of up to  $270^\circ$ .

Specifically, linear motion is achieved through the engagement of gear wheels with racks. The translational movement of the three linear axes is managed by THK linear recirculating ball guides, which feature four high-precision ground ball raceways and high rigidity due to the balanced configuration of the ball rings. The system utilizes Harmonic Drive epicyclic reducers, which, in the acquired geometric model, are represented as simplified steel blocks for computational efficiency. This abstraction is maintained to reduce geometric complexity and computational load while preserving the essential structural characteristics (see Figure 2 and Figure 3).

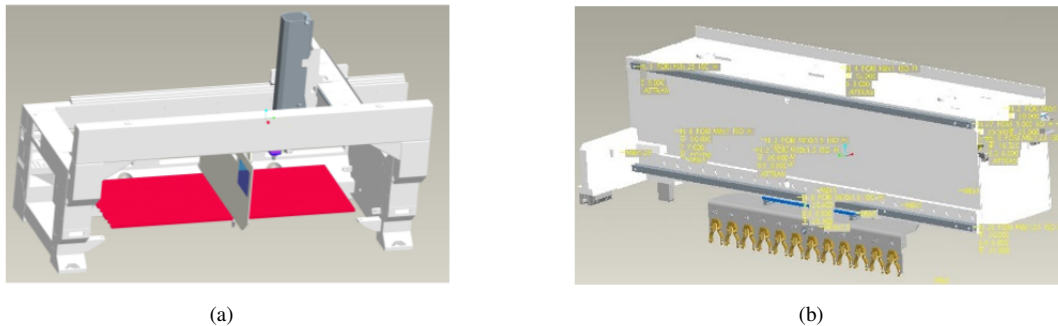


**Figure 2.** CAD models: (a) Overall system with the base evident; (b) Overhead carriage

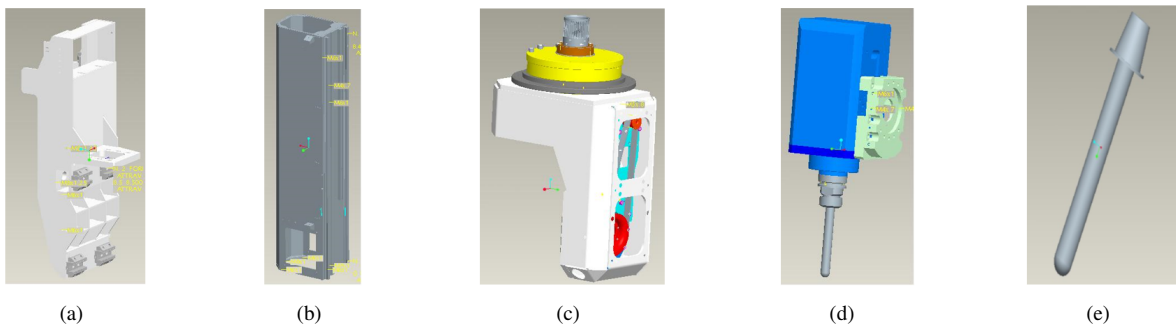


**Figure 3.** CAD models: (a) Y-axis carriage system; (b) Z-axis carriage system; (c) C-axis rotating system; (d) A-axis rotating system; (e) Representative cutting tool

However, beyond this preliminary simplification, the geometric complexity, quantity, and size of parts result in a significantly high computational cost, making it impractical to obtain a numerical solution. Consequently, it is necessary to develop customized geometric models tailored to specific load conditions. Additionally, CAD modifications are required, such as the removal of critical features (e.g., holes, fillets, and other intricate details) that complicate the discretization and solving processes. Once the most suitable geometric model has been defined, the *STEP* exchange format is used to import the geometry into the ANSYS workspace for further steps.

### 2.2.2 Mesh

The geometry is spatially discretized into finite elements (FE) and nodes, and the resulting mesh is validated. The meshing procedure follows an automatic discretization method, where the solver applies extrusion-based discretization when possible. If extrusion is not feasible, a *tetrahedral* decomposition has been used.

To enhance accuracy, refinement controls have been applied in regions requiring greater precision, and specific components can be assigned higher importance. This allows for localized adjustments in mesh fineness to improve numerical accuracy. A particular focus is placed on “*sweepable*” bodies, which are discretized using hexahedral elements (HEX), as they provide higher accuracy in simulation results.

The mesh dimension largely depends on the complexity of the components under investigation, as reported in the following examples (Figure 4):

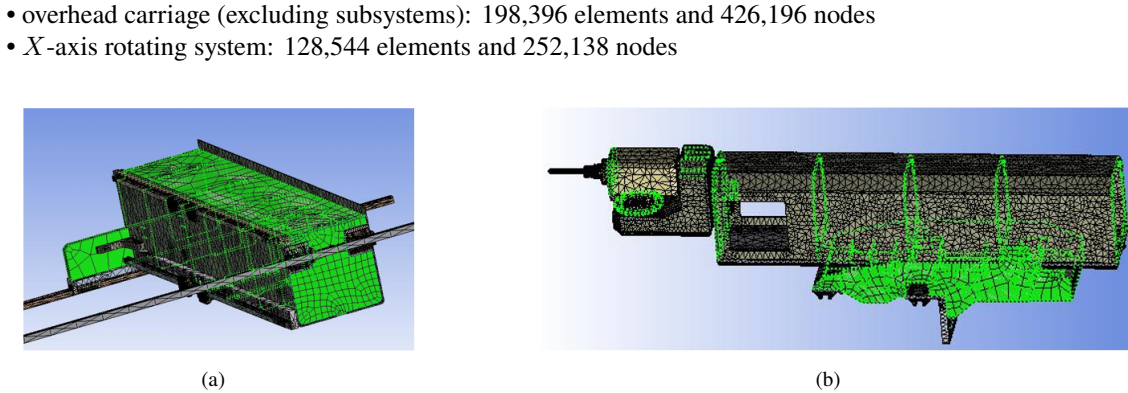


**Figure 4.** Discretization of main parts: a) Overhead carriage; b) X-axis rotating system

### 2.2.3 Materials

Each component is assigned to the most appropriate material. The structure is made entirely of structural steel, except for the worktop, made of aluminum alloy. All rails have been assigned C55 surface-hardening steel, selected for its ability to withstand significant wear caused by the rolling motion of the ball bearings in the linear guide carriages. The tool has been modeled using AISI 02 tool steel. Default material properties provided in the Ansys database have been retained without modifications. These values are summarized in Table 2.

**Table 2.** Material properties

Property	Structural Steel	Aluminum Alloy	Hardening Steel C55	AISI 02 Tool Steel
Young's modulus (GPa)	200	71	205	214
Poisson's ratio	0.30	0.33	0.29	0.30
Density (Kg/dm <sup>3</sup> )	7.85	2.77	7.85	7.83
Tensile yield strength (MPa)	250	280	560	1500
Compressive yield strength (MPa)	250	280	560	1500
Tensile breaking strength (MPa)	460	310	660	1690

### 2.2.4 Contacts

To ensure that assembly constraints closely align with real conditions, each contact area has been individually verified using contact controls that optimize the identification and management of such regions. Through a set of global settings, it is possible to define tolerance levels for contact size, as CAD-modelled assemblies may contain slight misalignments, such as small overlaps or gaps along the contact regions. Additionally, it is possible to specify the method of contact detection between different bodies. In the cases examined, face-to-face contact recognition is adopted.

Regarding the contact surfaces, when two surfaces of different bodies define a contact region, one acts as the “target” surface, while the other serves as the “contact” surface. For contact between rigid and flexible bodies, the target surface corresponds to the stiffer component, while the contact surface is assigned to the more flexible component. In cases involving contact between flexible bodies, selecting the correct surfaces is more complex, as an improper designation may lead to inconsistent penetration and affect the accuracy of the solution. To mitigate this issue, in the present analysis the following guidelines are applied:

- When a convex surface contacts a flat or concave surface, the flat/concave surface should be designated as the target surface.
- When one surface is significantly stiffer than the other, the softer surface should be set as the contact surface, while the stiffer one should be assigned as the target surface.
- When one surface is notably larger than the other, such as when one encloses the other, the larger surface should be designated as the target surface. Regarding the contact type, the selection of the appropriate contact type depends on the specific problem being addressed. Five different types of contact regions can be distinguished:
  - Constrained: The faces of the individual bodies are prevented from sliding or separating, making the region behave as if glued. This type of contact is suitable for linear solutions.
  - Non-separating: Similar to the previous type, except that small amounts of frictionless sliding can occur along the contact surfaces.
  - Frictionless: Models unilateral normal contact, meaning that the normal pressure is 0 if separation occurs. This solution is nonlinear, as the contact area can change based on the applied load. A friction coefficient of 0 is assumed, allowing free slip. The model must be well constrained to use this contact setting.
  - Rough: Similar to the frictionless type but enforcing infinite friction, preventing any slip between the contacting surfaces.
  - Frictional: Allows two contact faces to accumulate a given shear stress before slipping begins.

In the present analysis, the constrained contact type is generally adopted. Unlike other contact models, it does not introduce nonlinearity in the simulation, ensuring reasonable solution times and facilitating numerical convergence. This choice is motivated by the need to assess the general functionality of the adopted models and obtain an overall understanding of the machine's structural behaviour rather than focusing on detailed numerical accuracy. Where a higher level of precision, nonlinear contact models are also implemented (exceptionally) where necessary to improve numerical accuracy.

### 2.3 Impact Events

Types of impacts commonly encountered during normal operations of the machining center are the following:

1. Collisions with the work surface, due to errors in tool assembly, setup, or incorrect insertion depths. Both the spindle and the tool may strike the work surface, potentially leading to tool breakage.
2. Collisions during transfer phases, due to obstacles inadvertently left on the work surface that pose significant risks, especially if they are large or have rough surfaces. These objects become increasingly hazardous during rapid movements of the operating head, where higher speeds amplify kinetic energy and inertia, increasing the risk of severe impacts.
3. Collisions with obstacles or machine walls, due to unexpected movements involving the machine's rotary axes that may cause impacts with external obstacles or the machine's own structural elements. These collisions can occur as different parts of the machine operate within confined spaces or during specific machining processes.

Given this large variety of impact conditions, it is essential to establish predefined impact geometries that reflect the critical load settings. As first, it is assumed that:

- Although many impacts are noted on the rear side of the electrospindle, the impact scenarios considered in this study are based on the simplifying assumption that the impact zone is localized at the tool tip. This assumption is adopted because it poses the most significant risk to the structure, with impact loads applied at a longer lever arm, resulting in increased torsional and bending moments.

- To adequately model the impact phenomenon, a specific representative tool is attached to the electrospindle. Designed to simulate a longer and slenderer tool, typically used in the machine, it has dimensions of 160 mm in length and 20 mm in diameter, resembling a cylindrical body (The subgraph (e) of Figure 3). Its dimensions help to realistically represent the conditions under which the machine operates during impacts.

The most critical impact geometries that will represent the load conditions during the simulation are (Figure 5):

1. Vertical Impact – the spindle is aligned to the “Z” axis, with movement occurring along the vertical axis (case 1).
2. Transverse Impact – the spindle remains aligned along the “Z” axis, but the motion occurs in the X – Y plane (case 2).
3. Diagonal Impact – the spindle is inclined by 45° with respect to the “Z” axis, and the motion takes place vertically, similar to the first case (case 3).
4. Rotating Impact – the spindle axis remains inclined at 45° relative to the “Z” axis, but the impact results from the rotation of the rotary axis “A” (case 4).

These scenarios are chosen for their potential to impose the most severe conditions on the machine's structure, making them focal points for detailed study and simulation. The simulation is tailored to account for the rapid speeds at which the machine's operating head moves, which are critical for assessing the impacts under operational speeds. The reference speed data for these simulations is reported in Table 3.

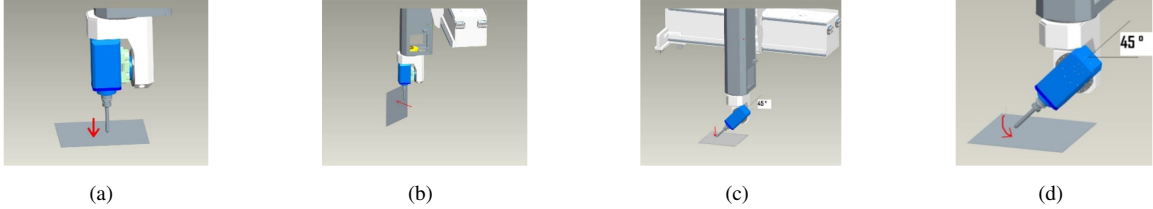


**Figure 5.** Geometrical impact conditions: (a) Vertical; (b) Transverse; (c) Diagonal; (d) Rotating impacts

**Table 3.** Representative speeds

Movement Type	Axis	Speed			
		m/min	m/s	rpm	rps
Horizontal Rapid Traverse	X-axis, Y-axis	100	~1.65		
Vertical Rapid Traverse	Z-axis	75	~1.25		
Rotary Rapid Motion	C-axis, A-axis	33	~0.50		

#### 2.4 Analysis Type

Since experimental data on dynamic impact events (e.g., impact duration) is unavailable, a static equivalent approach based on controlled deformation was preferred. In this method, predefined displacements were imposed on critical areas to replicate the effects of sudden impact forces, providing a computationally efficient alternative to force-based impact modelling. This approach allowed for a realistic estimation of stress and strain distributions within the machine structure while making it easier to isolate and identify structural weak points. By analyzing stress concentrations and deformation patterns, vulnerable areas were pinpointed, particularly in load-bearing components such as the overhead carriage, linear guides, and rotary axes. These insights offer valuable guidance for design improvements, including reinforcing critical parts or introducing localized energy-absorbing elements to mitigate impact effects.

Specifically, based on feedback from technical support services, two impact scenarios have been considered as middle-intensity impacts, corresponding to the displacement of the tool tip, here expressed with respect to the vertical axis (Z-axis) (Figure 6):

- Transverse impact with a displacement of 5 mm
- Axial impact with a displacement of 3 mm

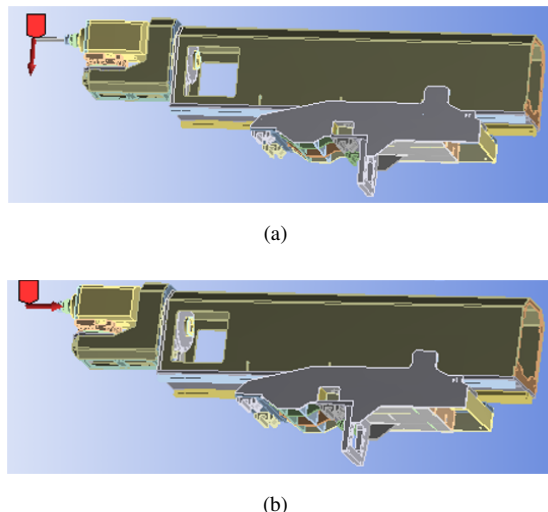


**Figure 6.** Impact scenarios: (a) Transversal impact; (b) Axial impact

Based on the results achieved by imposing deformations, an iterative approach has been used to determine the impact force that, if applied statically, would produce an equivalent deformation. For the purpose, further simplifications have been introduced sometimes, such as assuming that the impact occurs against infinitely rigid surfaces (e.g., the basis) and is elastic (no energy dissipation). Despite these and other simplifications, in cases

where a comparison between real-world data and simulation has been possible, the results have shown no significant discrepancy.

### 3 Results and Discussion

#### 3.1 Transverse Impact

The transverse impact, equivalent to an imposed displacement of the tool tip by 5 mm, was analysed under three different impact scenarios (Figure 7):

- Frontal direction, with displacement backward.
- Rear direction, with displacement forward.
- Lateral direction, with displacement sideways in the opposite direction.

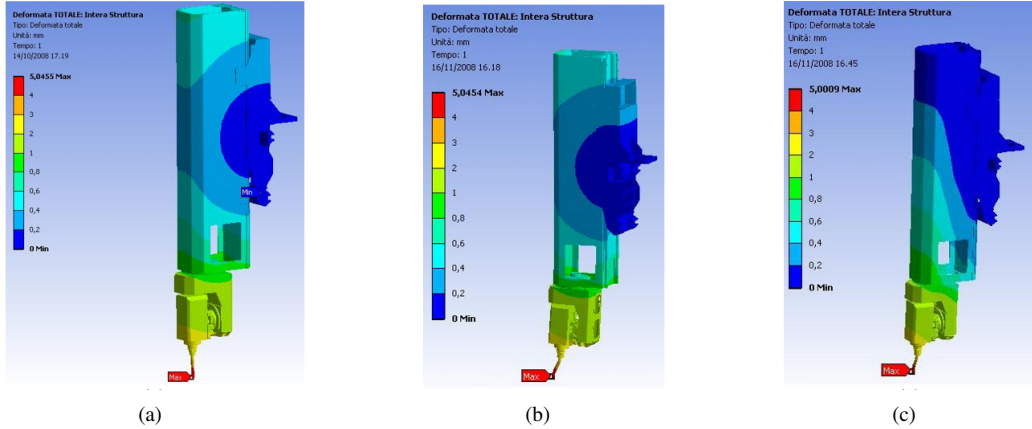


**Figure 7.** Transverse impact in (a) Frontal, (b) Lateral directions

For each of these three scenarios, Figure 8, Figure 9, and Figure 10 show the equivalent (*VonMises*) stresses in the cases of some of the most relevant structures, specifically (a) C-axis rotating system; (b) Y/X sliding pads; and (c) Y/Z sliding pads. Considering the material properties (Table 2) and the fact that the sliding pads are in hardening steel, it becomes evident that, while localized yielding occurs in certain areas, the ultimate tensile stress is never reached.

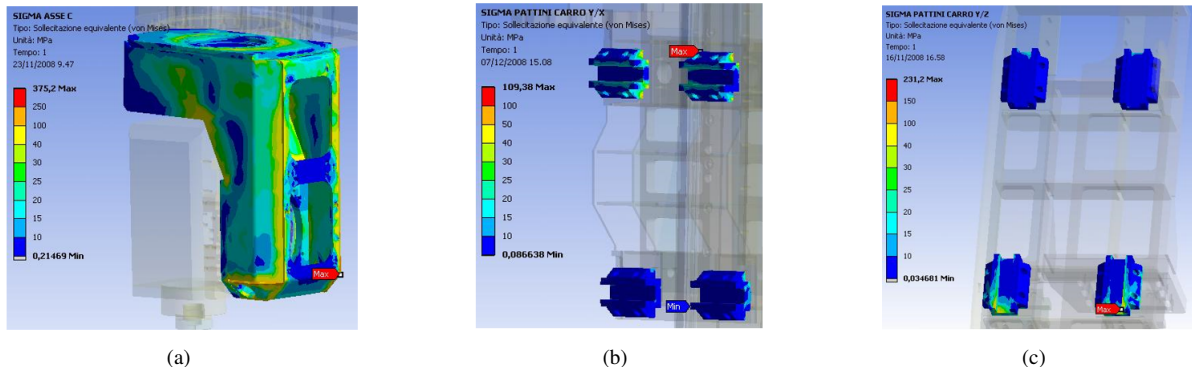


**Figure 8.** Transverse impact in frontal direction: (a) C-axis rotating system; (b) Y/X and (c) Y/Z sliding pads

#### 3.2 Axial Impact

The axial impact, equivalent to an imposed displacement of the tool tip by 3 mm upward, was analysed under two different impact scenarios:

- Vertical direction, with the spindle vertically aligned (at 0°) to the vertical axis.
- Vertical direction, with the spindle inclined (at 45°) with respect to the vertical axis.

For the two cases, Figure 11 and Figure 12 show the equivalent (*VonMises*) stresses, focusing, as before, on the same representative parts, specifically (a) the C-axis rotating system; (b) Y/X sliding pads; (c) Y/Z sliding pads.

Considering the material properties (Table 2), it is evident the ultimate tensile stress is reached, and parts' failure occurs.

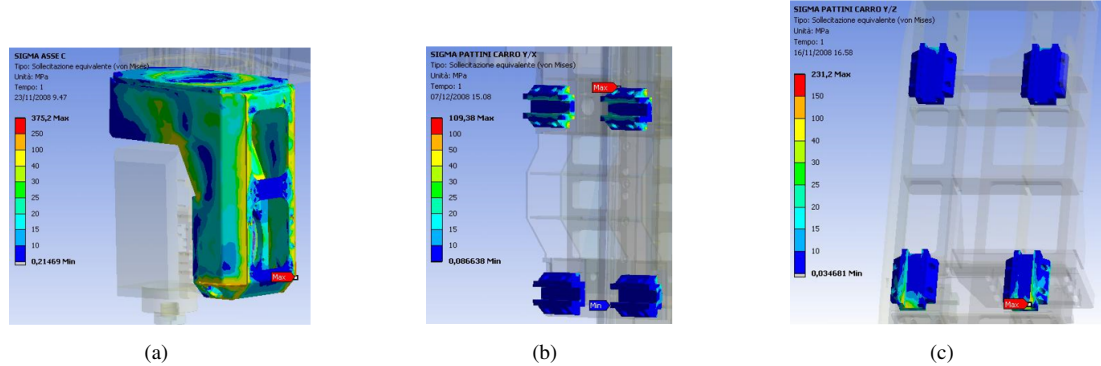


**Figure 9.** Transverse impact in frontal direction: (a) C-axis rotating system; (b) Y/X and (c) Y/Z sliding pads

### 3.2.1 Load estimation

Starting from the tool displacement value, as imposed during the preliminary FEM simulations, the magnitude of the impact loads ( $P$ ) can be determined iteratively thanks to further static simulations. Figure 13 represents, i.e., the case of transverse impact in a frontal direction with displacement backward (case a in par. 3.1). The system here is simplified by a cantilever beam subjected to a horizontal force ( $P$ ) applied at its free end. The beam is fixed at the top, meaning it is fully constrained at that point. The Young's modulus ( $E$ ) and cross-sectional area ( $A$ ) remain approximately unchanged during the impact. The system exhibits a linear response since, by design, no non-linearity has been introduced into the numerical model so far (e.g., non-linearities related to contacts, materials, or displacements). As a result, a straight line can represent the relationship between force and displacement, allowing the required force of 4175 N to generate the imposed displacement of 5 mm to be easily derived.

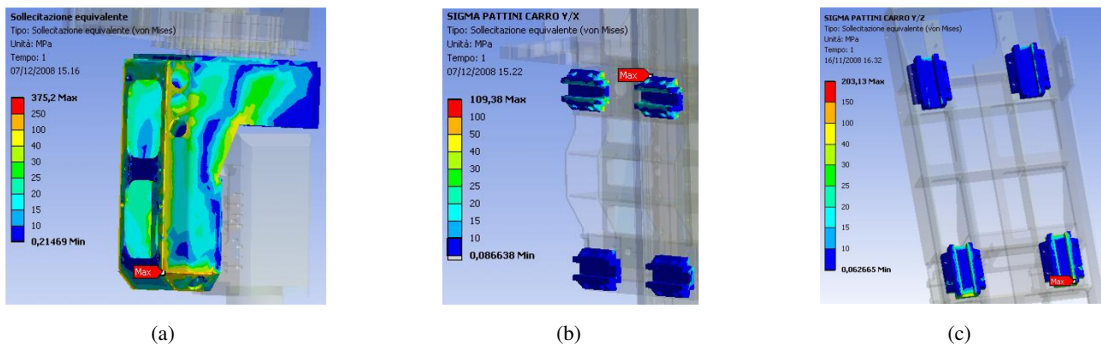


**Figure 10.** Transverse impact in frontal direction: (a) C-axis rotating system; (b) Y/X and (c) Y/Z sliding pads

Analyzing the different impact scenarios under investigation, results such as those reported in Table 4 have been obtained. Limiting the discussion to the three components already considered, the table offers a quick estimation of loads and stresses present in different critical areas of the system.

At the same time, the procedure also offers a way to provide an in-depth analysis with respect to specific situations (Table 5). For instance, as reported in similar investigations (e.g., the study [16]), results from simulation permit to highlighting how critical supports can be. Specifically:

- in the current configuration of linear guides between the Y and X carriages, the bearings located on the upper side tend to be more stressed.
- in the guide system between the Y and Z carriages, the bearings on the lower side experience the highest stress.
- the bearings of the overhead carriage are not affected by impact forces.
- in the C rotary axis, localized areas with high stress concentration are observed, particularly near the weld joints.

Or, in the case of each relevant component under investigation, such as the overhead carriage, it can provide detailed information about the stress/strain states (as shown in Figure 14).

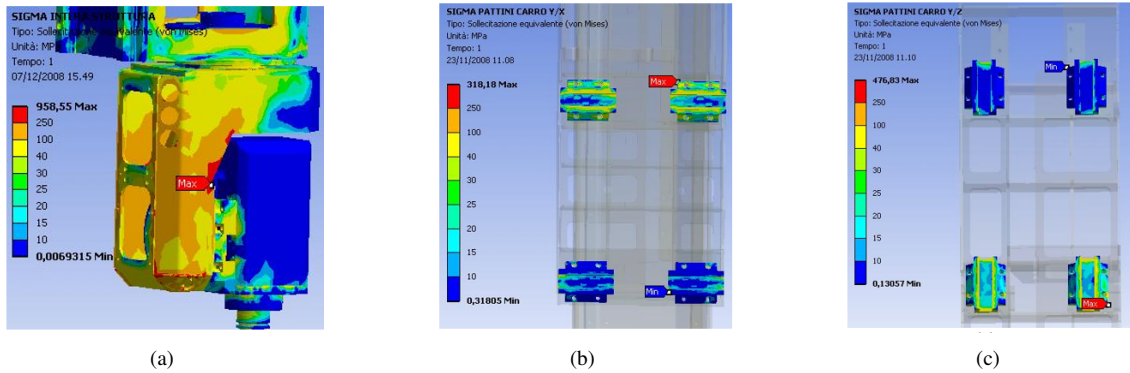


**Figure 11.** Axial impact with spindle aligned: (a) C-axis rotating system; (b) Y/X and (c) Y/Z sliding pads

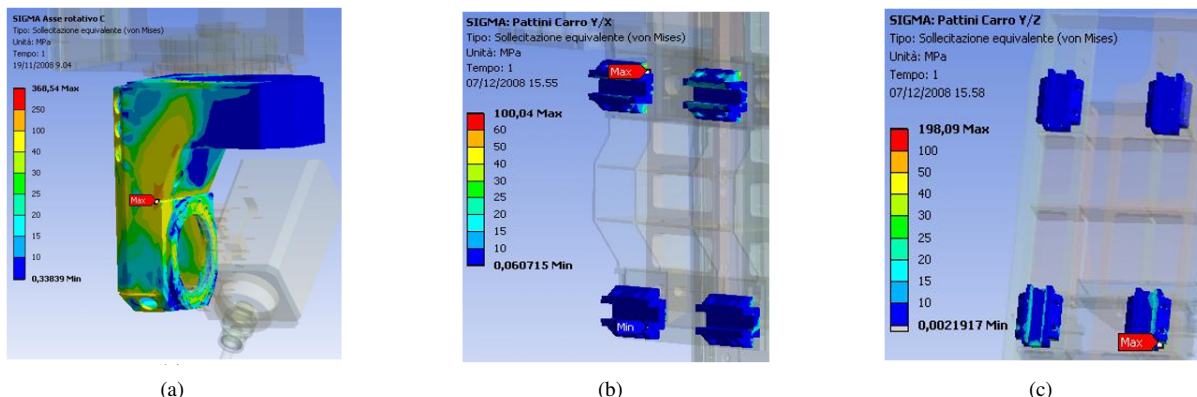


**Figure 12.** Axial impact with spindle not aligned: (a) C-axis rotating system; (b) Y/X and (c) Y/Z sliding pads

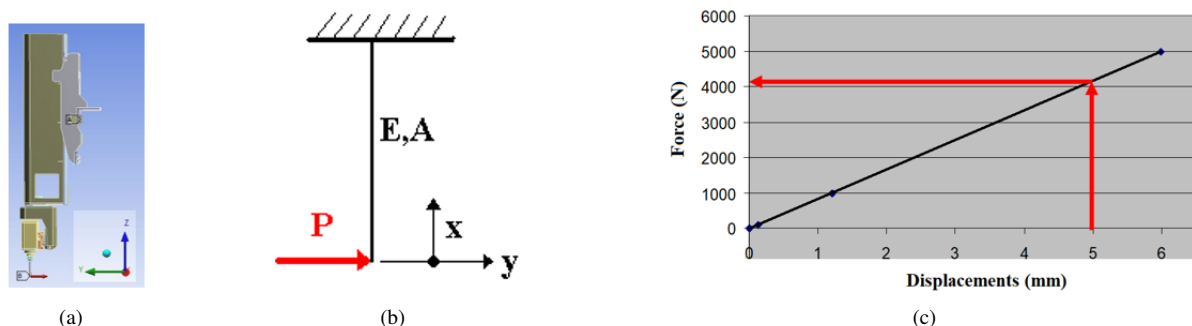


**Figure 13.** Load estimation: (a) Impact configuration; (b) Representation; (c) Force/displacement relation

**Table 4.** Load and stress

Impact	Direction	Impact Force	Y/Z Sliding Pads	Y/X Sliding Pads	C-axis Rotating System
			kN	MPa	MPa
Transverse	Frontal	4.2	110	375	110
	Rear	3.8	110	375	110
	Lateral	3.5	100	280	100
Axial	Vertical	100	320	950	320
	Inclined	77	100	370	100

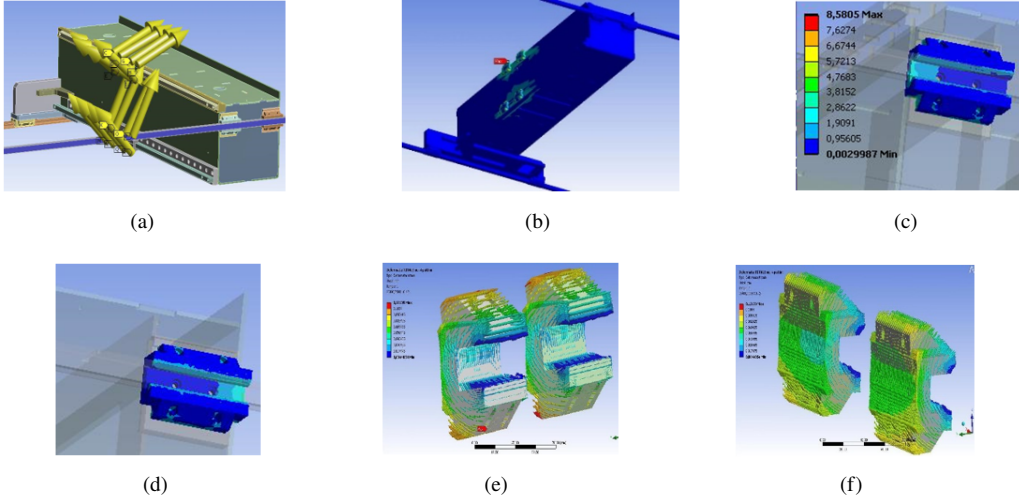


**Figure 14.** Overhead carriage FEM analysis: (a) Intensity and directions of forces; (b) General stress state; front (c) and (d) Rear support systems; Upper (e) and Lower (f) Varriage X/Y pads

**Table 5.** Guidelines for structural redesign

Impact	Direction	Y/Z Sliding Pads	Y/X Sliding Pads	C-axis Rotating System	Suggested Improvements (Illustrative Examples)
Transverse	Frontal	✓		✓	Enhance joints to reduce localized stress
	Rear	✓		✓	Add structural supports to dissipate energy
Axial	Lateral	✓	✓		Optimize lateral guides for impact absorption
	Vertical	✓✓	✓✓	✓✓	Use higher fatigue-resistant materials
	Inclined	✓	✓	✓	Improve bearing supports for better stability

#### 4 Conclusions

The present study has enabled an in-depth analysis of the behavior of a CNC machining center under impact conditions. By adopting a simplified, static approach, it was possible to investigate different impact scenarios and identify the components most affected by impact forces. The findings indicate that vertical impacts primarily affect the tool rather than the overall machine structure, while skates positioned on the overhead crane remain largely unaffected. In the configuration involving linear guides between the Y and overhead carriage, the upper-side skates experience the highest stress levels, whereas in the linear guide configuration between the Y and Z carriage, the lower front pads are the most impacted. Additionally, the rotary axis C exhibits localized areas of high stress concentration, particularly near the welded joints of its subsystem.

A set of reusable simulation models has been developed as well, enabling future studies. In these terms, significant challenges were encountered in defining appropriate boundary conditions for isolating critical components. A methodology for separating specific details from global simulations was proposed, revealing that upper pads are subjected to greater stress than lower ones. Despite these insights, the results are subject to a high degree of approximation due to the simplifying assumptions required by the static approach.

Given the limitations of static analysis, future research should focus on dynamic simulations, which better reflect the nature of impact events. However, such analyses require high-performance computational resources to account for nonlinear effects, including contact interactions and material behavior. To achieve a more comprehensive understanding of crash-related issues, implementing simulations using the ANSYS LS-DYNA module is recommended. Additionally, further studies could extend the analysis to the remaining guidance systems of the machine, including rotary components, once their contact and load conditions are clearly defined.

## Author Contributions

Conceptualization, C.F.; methodology, A.P. and C.F.; software, S.P. and A.P.; validation, D.M. and A.P.; formal analysis, C.P. and S.P.; investigation, S.P. and A.P.; resources, C.F.; data curation, A.P.; writing—original draft preparation, S.P. and C.F.; writing—review and editing, C.F. and D.M.; visualization, A.P. and D.M.; supervision, C.F.

## Data Availability

The data used to support the research findings are available from the corresponding author upon request.

## Acknowledgements

The authors acknowledge Eng. Giovanni Iezzi (SCM Group Spa) for his indispensable support, including his efforts to share machine models and other confidential information. Additionally, AI-based language enhancement tools were used to improve the clarity and fluency of this document.

## Conflicts of Interest

The authors declare no conflict of interest.

## References

- [1] J. Marek, *Design of CNC Machine Tools*. MM Publishing, SR O., 2015.
- [2] M. A. Mamadjanovich, S. M. Yusupov, and S. Sadirov, “Advantages and the future of CNC machines,” *Sci. Prog.*, vol. 2, no. 1, pp. 1638–1647, 2021.
- [3] A. Pavlovic and C. Fragassa, “Analysis of flexible barriers used as safety protection in woodworking,” *Int. J. Qual. Res.*, vol. 10, no. 1, pp. 71–88, 2016. <https://doi.org/10.18421/IJQR10.01-03>
- [4] S. H. Suh, S. K. Kang, D. H. Chung, and I. Stroud, *Theory and Design of CNC Systems*. Springer Science & Business Media, 2008.
- [5] G. Lucisano, M. Stefanovic, and C. Fragassa, “Advanced design solutions for high-precision woodworking machines,” *Int. J. Qual. Res.*, vol. 10, no. 1, pp. 143–158, 2016.
- [6] M. Soori, F. K. G. Jough, R. Dastres, and B. Arezoo, “Sustainable CNC machining operations, a review,” *Sustain. Oper. Comput.*, vol. 5, pp. 73–87, 2024. <https://doi.org/10.1016/j.susoc.2024.01.001>
- [7] B. M. Swami, K. S. R. Kumar, and C. H. Ramakrishna, “Design and structural analysis of CNC vertical milling machine bed,” *Int. J. Adv. Eng. Tech.*, vol. 3, no. 4, pp. 97–100, 2020.
- [8] A. Andoko, R. Wulandari, R. Prasetya, R. P. Jeadi, D. R. Pradica, P. Kurniawan, A. D. Putra, G. A. Kurniawan, and S. Kamaruddin, “Simulation of CNC milling 5 axis with finite element method,” vol. 2262, no. 1, p. 040013, 2020. <https://doi.org/10.1063/5.0015746>
- [9] V. I. Guzeev and A. K. Nurkenov, “Researching the CNC-machine stiffness impact on the grinding cycle design,” *Procedia Eng.*, vol. 150, pp. 815–820, 2016. <https://doi.org/10.1016/j.proeng.2016.07.118>
- [10] X. H. Yang and K. Cheng, “Investigation on the industrial design approach for CNC machine tools and its implementation and application perspectives,” *Procedia Manuf.*, vol. 11, pp. 1454–1462, 2017. <https://doi.org/10.1016/j.promfg.2017.07.276>
- [11] E. Csandy, Z. Kovcs, E. Magoss, and J. Ratnasingam, *Optimum Design and Manufacture of Wood Products*. Cham, Switzerland: Springer International Publishing, 2019.
- [12] M. Soori and B. Arezoo, “Modification of CNC machine tool operations and structures using finite element methods, A review,” *Jordan J. Mech. Ind. Eng.*, vol. 17, no. 3, pp. 327–343, 2023. <https://doi.org/10.59038/jjmie/170302>
- [13] S. Group, “ROUTECH Chronos HT Machine Tool,” 2023. <https://www.youtube.com/watch?v=xWtZIVll8gc>
- [14] S. G. Racz, R. E. Breaz, and L. I. Cioca, “Hazards that can affect CNC machine tools during operation—An AHP approach,” *Safety*, vol. 6, no. 1, pp. 10–18, 2020. <https://doi.org/10.3390/safety6010010>
- [15] T. Stolarski, Y. Nakasone, and S. Yoshimoto, *Engineering Analysis with ANSYS Software*. Butterworth-Heinemann, 2018.
- [16] K. Gok, E. Turkes, S. Neseli, and Y. Kisiolu, “Failure analysis of support during profile cutting process using horizontal milling machine,” *Int. J. Adv. Manuf. Technol.*, vol. 70, pp. 1169–1179, 2014. <https://doi.org/10.1007/s00170-013-5356-4>